https://doi.org/10.5194/egusphere-2023-397
Preprint. Discussion started: 14 March 2023

Hydrothermal activity of the Lake Abhe geothermal field (Djibouti): Structural controls and paths for further exploration

Bastien Walter[1], Yves Géraud[1], Alexiane Favier[1], Nadjib Chibati[1], Marc Diraison[1]

[1] Université de Lorraine, UMR 7359 GeoRessources, École Nationale Supérieure de Géologie, 2 Rue du Doyen Marcel Roubault, Vandoeuvre-lès-Nancy 54518, France

Correspondence to: Bastien Walter (bastien.walter@protonmail.com); Yves Géraud (yves.geraud@univ-lorraine.fr)

Abstract. Lake Abhe is sitting on the Gob Aad graben within the tectonic Afar triangle in the Republic of Djibouti. It is known for its exposures of massive hydrothermal chimneys on the lake's eastern shore. The many hydrothermal surface manifestations on this side of the lake, including steam vents, hot springs and carbonate chimney structures, reflect the geothermal field of this area. This study describes the structural settings of the Lake Abhe Geothermal Field (LAGF), using multiscale structural lineament distribution mapping. It also investigates the hydrothermal surface manifestations distribution in order to specify structural controls on local fluid flow and discuss its evolution. Structural features of the LAGF area are dominated by ESE-trending extensional faults that form a series of narrow elongated horst, graben and half-graben structures. Fault interaction and accommodation zones, as well as fault intersections, relay ramps and possible breaching faults are also recognized and may represent interesting structural features in terms of fluid flow pathways. Hydrothermal chimneys and hot springs distribution over the LAGF area is controlled by the main structural trends, and show signs of higher hydrothermal activity located at intersecting structural traces. Field observations, in conjunction with satellite images analysis, suggest a progressive lateral evolution of the LAGF hydrothermal fluid outflows over time. Therefore, this study provides new insights on the local tectonically driven fluid flow of the LAGF, that may support further exploration of this remarkable site and may promote its geothermal development.

1 Introduction

Africa, in particular along the Eastern African Rift System (EARS), offers significant geothermal potential, providing great opportunities for these countries to reinforce their energy mix with renewable energy (IRENA, 2020). With Kenya leading a strong regional dynamic, being the fifth country worldwide having the most installed geothermal power generation capacity in 2020 (1.193 MWe; (Huttrer, 2021)), many countries of eastern Africa are now engaged in the exploration and development of this renewable energy resource (ARGeo, 2022).

Geothermal systems provide an opportunity for permanent and flexible power production in a large variety of environments. These systems can be distinguished based on their temperature, between high (>150°C), medium (between 150 and 100°C) and low (<100°C) enthalpy resources (Moeck, 2014;

https://doi.org/10.5194/egusphere-2023-397
Preprint. Discussion started: 14 March 2023

Stober and Bucher, 2021). While the development of geothermal energy has long been focused on high enthalpy systems producing a high energy yield, technological advances allowed a more efficient exploitation of the entire range of geothermal resources for electricity production as well as heat direct-use (Rubio-Maya et al., 2015).

Considering some of the region's socio-economic challenges, with 59% of the Sub-Saharan African population living in rural areas and only 28.5% of said population having access to electricity in 2020 (World Bank, 2023a, 2023b), several projects are now aiming to develop adapted geothermal solutions. They correspond to autonomous geothermal small-scale systems designed for African communities considered as "off-grid" (i.e. not connected to a power grid). These solutions are based on the analysis of the needs of these local populations in terms of geothermal direct-use, and can include small-scale Organic Rankine Cycle technology for local electricity production. The 'Geothermal Village' (GV) project, implemented within the framework of the LEAP-RE project and financed by the Horizon 2020 program for research and innovation of the European Union, is intended for such remote communities in the Republic of Djibouti (Varet et al., 2020).

The Republic of Djibouti, located on the north-eastern end of the EARS, represents an interesting area for studying hydrothermalism in the context of intracontinental extension. Assessments of geothermal systems worldwide have highlighted the critical role of fault and fracture systems on the near surface permeability (Jolie et al., 2021). The country is sitting on the tectonic Afar triangle and exhibits a complex fragmented relief, composed of high blocks and grabens, and a widespread geothermal activity (e.g. hot springs, fumaroles, hydrothermal alteration). These structures are mainly located in the western part of the country and along the Gulf of Tadjourah ridge (Gall et al., 2018). The Asal-Ghoubbet rift area has been significantly studied in order to characterize the Lake Asal geothermal field (D'Amore et al., 1998; Houssein and Axelsson, 2010; Abdillahi et al., 2016). However, due to remote and poorly accessible sites, other potential geothermal areas remain relatively unexplored. The Lake Abhe Geothermal Field (LAGF), located on the southwestern edge of the Republic of Djibouti along the Gob-Aad graben is one of these area (Dekov et al., 2014; Awaleh et al., 2015).

This paper aims to shed light on one of these remote geothermal systems. Using remote sensing datasets and field observations, we present here a multiscale structural survey and a lineament distribution mapping, carried out in order to specify the structural settings of the LAGF. This paper also provides insights on the structural control on the LAGF fluid flow, based on the hydrothermal surface manifestations analysis observed in this area.

2 Geological setting

Lake Abhe is located on the southwestern edge of the Republic of Djibouti, on the border with Ethiopia. The lake sits near the center of the triple rift junction of Red Sea and Gulf of Aden oceanic rifts with the continental East African rift system (EARS), also known as the Afar Triangle (Chorowicz, 2005) (Fig. 1). The lake occupies the western end of the Gob Aad closed tectonic basin, an ESE-WNW striking asymmetrical graben that connects to the larger NNW-SSE striking Tendaho graben, in the vicinity of the Dama Ale volcano (Beyene and Abdelsalam, 2005; Polun et al., 2018). The Gob Aad graben shoulders found in the Lake Abhe area are composed of the 1 to 4 My basalt Stratoid Series, which

https://doi.org/10.5194/egusphere-2023-397
Preprint. Discussion started: 14 March 2023

dominates the surface geology of the central Afar region (Deniel et al., 1994; Beyene and Abdelsalam, 2005, Michon et al., 2022). These volcanic units are affected by a pervasive ESE-WNW striking normal faults system that forms a horst – graben network outcropping northeast to the lake (Demange et al., 1971). The basin is filled by Lower Pleistocene - Holocene lacustrine and detrital sediments, slightly deformed and post-dating the normal fault system. These sediments marked the successive periods of climate changes and significant lake-level variations. The lake-level evolution from the past 70 ky underwent successive transgressions with high-water level fluctuating by almost 200 m, with Holocene episodes of highstand identified at about 10-8 ky and 7.5-4 ky (Gasse, 1977; Gasse and Street, 1978; Khalidi et al., 2020). The modern lake surface has an elevation of about 240 m above sea level, but varies seasonally by a few meters depending on river water input. This lake is currently a closed basin, highly alkaline (pH=9.86) and hyper-saline (total dissolved solids >90,000 mg/L) (Awaleh et al., 2015). The Lake Abhe eastern shore is particularly rich in hydrothermal surface manifestations, including steam vents, hot springs and hydrothermal chimney structures, spread over an area of about 100 km^2 (Houssein et al., 2013; Dekov et al., 2014). The latter structures, exposed thanks to the recent lake shrinking over the unconsolidated sedimentary flats, make this area remarkable. These carbonate chimneys extend over about 5 km between the lake shoreline and the surrounding basalt hills to the east, as individual structures or as clusters. Inter-chimney materials consist of unconsolidated mixed carbonate and siliciclastic mud, with localized weakly-lithified diatomites and mudstones (DeMott et al., 2021). These features are generally aligned in an ESE-trend, reflecting the regional fault network main direction. The chimney field is generally subdivided in the existing literature into two fields separated by a small wadi: the Small Hydrothermal Chimneys area (SHCa) in the north and the Great Hydrothermal Chimneys area (GHCa) in the south. Chimneys in the north show more lateral continuity and are commonly a few meters high, whereas those in the south are more isolated and higher, up to a few tens of meter (Fig. 1). These hydrothermal chimneys have been extensively described at the macro-, meso- and micro-scale by DeMott et al. (2021) in terms of morphology, texture and fabric. They exhibit a variety of large-scale (meter to decameter) morphology, classified as massive, pinnacle, bulbous, barrel or frondose. Carbonate chimneys are commonly characterized by a high number of cm- to dm-scale tubular crystalline structures growing upward and/or outward from the chimney bases, and of cavities of similar scale, forming overall dendritic and/or honeycomb textures. At the micro-scale, these highly porous and friable structures are mostly composed of calcite with needle-like, sugar-like and / or dendritic fabrics, and with relatively little pore infilling except for minor amounts of evaporites. A 3-5 cm thick stromatolitic crust that coat the external surface of the chimneys is generally described. Despite differences in terms of morphology and distribution between the two sub-fields, all the Lake Abhe chimneys are interpreted to have been formed during the last few tens of thousands of years as abiogenic products of mixing between hydrothermal sublacustrine springs and lake waters during lake highstand intervals (DeMott et al., 2021). Numerous hot springs (T: 70-100°C) found at the base of chimneys and hot steam vents at their apex reveal the current hydrothermalism of this area (Awaleh et al., 2015). Hot springs generally form small ponds, partly irrigated, that are surrounded by vegetation that benefits the local fauna and pastoral communities.

https://doi.org/10.5194/egusphere-2023-397
Preprint. Discussion started: 14 March 2023

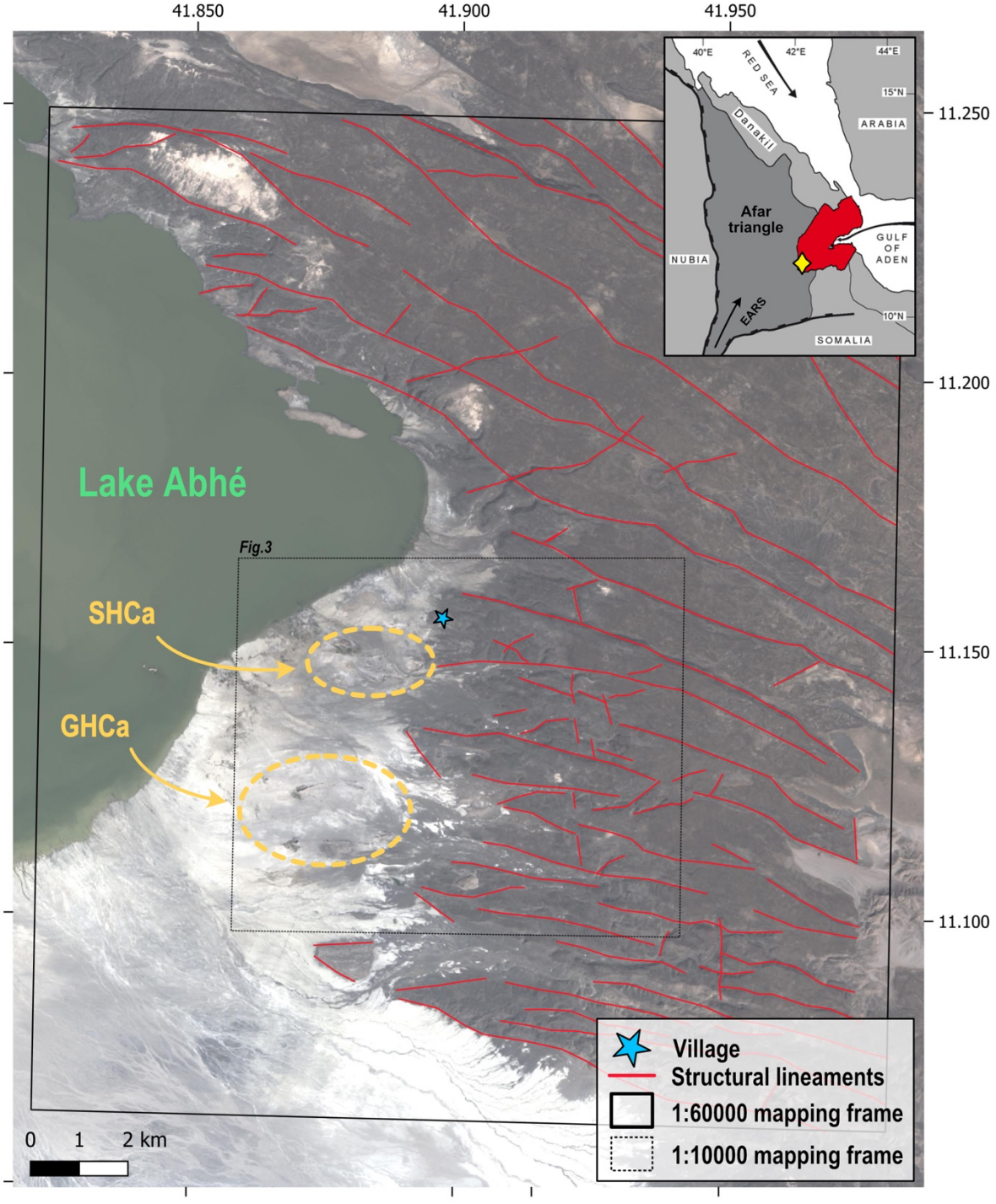

Figure 1: Location map of the LAGF and the two Small Hydrothermal Chimneys area (SHCa) and Great Hydrothermal Chimneys area (GHCa). 1/60,000 scale structural lineament mapping results are represented as red lines. Inset map indicates the study area location at the regional scale (adapted after Awaleh et al., 2018).

https://doi.org/10.5194/egusphere-2023-397
Preprint. Discussion started: 14 March 2023

The LAGF is one of the geothermal prospect areas of the Republic of Djibouti that benefited from surface exploration surveys (Demange et al., 1971; Moussa and Souleiman, 2015; Abdillahi et al., 2016). As part of geothermal energy development programs, Djiboutian national institutions (ODDEG, CERD) initiated geological, geochemical and geophysics surveys that led to the definition of a reservoir model of the LAGF with the support of international organizations (Fahman et al., 2018; Samod et al., 2018). According to Awaleh et al. (2015), the LAGF reservoir is mainly fed by meteoric water that penetrates downwards through the fracture network in the basalt Stratoid Series and combine with deep regional groundwater in the thermal aquifer to a maximum depth of about 1 km. Reservoir temperatures estimated from geothermometers range between 120 and 160°C, with a mean temperature of about 135°C. Exploration work of the LAGF concluded to a medium-enthalpy geothermal system that could benefit from small-scale stand-alone electric production systems and/or in cascade thermal direct-use (Moussa & Souleiman, 2015; Varet et al., 2020).

3 Methods

A field campaign focused on the SHCa and the basalt Stratoid Series outcropping east to these chimneys was conducted in November 2021. The fieldwork on the volcanic rocks consisted in the petro-structural characterization of the surrounding basalt series in terms of analog reservoir and fluid flow key features (i.e. faults, fractures, hydrothermalized zones, etc.). A structural survey of plurimetric fractures affecting the chimneys of the SHCa was carried out, with tens of chimneys and hot springs observed in this area. An imaging and topographic survey of the SHCa was conducted with a DJI Phantom 4 Pro drone and adjacent topographic datasets and images were merged using QGIS.
As part of the structural survey of the studied area, structural lineaments were mapped using high-resolution remote sensing data and interpreted with knowledge acquired from field geological observations. Detailed lineament mapping was carried out on two digital elevation model (DEM) displayed on QGIS Version 3.22.6, using two different fixed viewing scale depending on the DEM resolution. The NASA Shuttle Radar Topography Mission (SRTM) Global 1 arc second DEM (~30m resolution) was used to map lineaments at the displaying scale of 1/60000 over a large area (NASA JPL, 2013). Focused on the main hydrothermal active area, a higher resolution DEM (0.5m resolution) was generated from PLEIADES tri-stereo multispectral (MS) satellite imagery. This DEM was used to map structural lineaments of the volcanic series and hydrothermal chimneys alignments separately at the displaying scale of 1/10000. Rose diagrams representing lineament mapping results were generated with the *Line Direction Histogram* QGIS plugin (Tveite, 2015), with the lineament orientation distribution in intervals of 10°. The length of the single bins of these diagrams corresponds to the number of lineaments occurring in each of these intervals, weighted by the lineament's length. Hot springs outflowing over the sedimentary flats of the LAGF area were mapped using color-saturated GoogleEarth images (© Google Earth 2022). Hot springs were identified thanks to the green vegetation surrounding small ponds clearly visible on these images, based on field observations knowledge.

https://doi.org/10.5194/egusphere-2023-397
Preprint. Discussion started: 14 March 2023

4 Results

4.1 Multi-scale lineament mapping

4.1.1 1:60,000 scale mapping of structural lineaments

90 structural lineaments were mapped using a 1/60000 viewing scale, over an area of about 361 km^2 centered on the LAGF (Fig. 1). The average length of the lineaments is 3074 m, with a maximum length of 17.1 km, although 14 of these lineaments are cut by the mapping frame. The strongly dominant lineament direction is ESE-WNW (090 to 120°) (Fig. 2a). Minor sets of ENE-WSW (070 to 090°), SE-NW (120 to 140°) and N-S (170 to 180°) oriented lineaments are also observed. ENE- and SE-trending lineaments are rather highlighted north of the mapping area by the hydrographic network descending the Gob Aad graben shoulder. N-S oblique lineaments are observed through the Stratoid Series outcropping east of the LAGF.

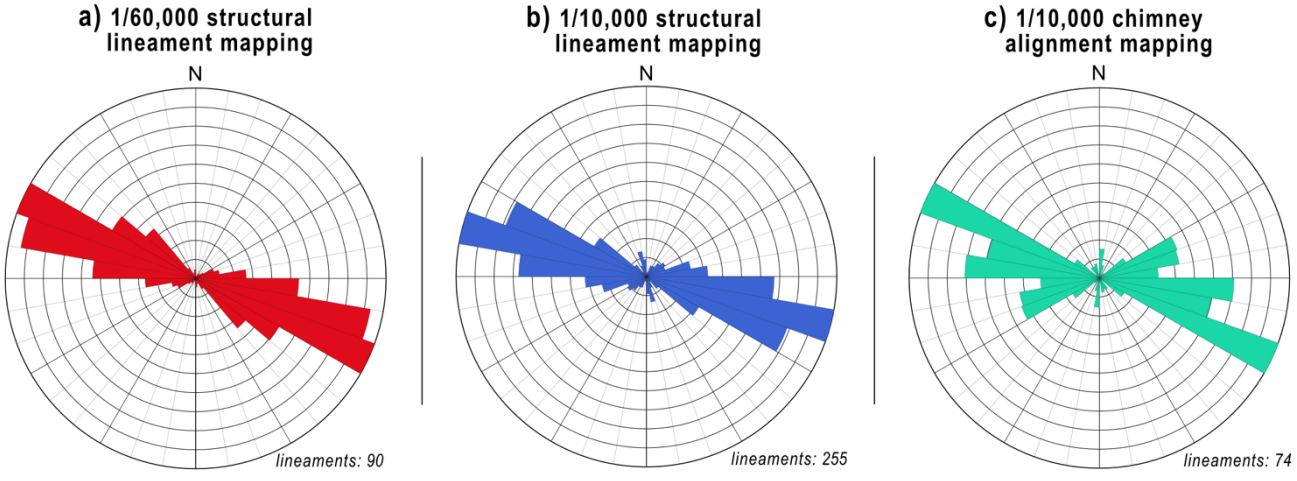

Figure 2: Rose diagrams representing: a) 1/60,000 scale structural lineament mapping, b) 1/10,000 scale structural lineament mapping and c) 1/10,000 scale hydrothermal chimney alignment mapping.

4.1.2 1:10,000 scale mapping of structural lineaments and hydrothermal chimneys alignment

255 structural lineaments were mapped at a 1/10000 viewing scale within the Stratoid Series hills east to the LAGF (Fig. 3). The average length of the lineaments is 541 m, with a maximum length of 4.6 km, although 17 of these lineaments are cut by the mapping frame. The strongly dominant lineament direction is ESE-WNW (090 to 120°) (Fig. 2b). Similar to this main direction, two secondary direction of ENE-WSW (070 to 090°) and SE-NW (120 to 140°) oriented lineaments are observed and form dihedral pattern well visible west nearby the contact with the sedimentary flats. Minor sets of oblique N-S (160 to 180°) and NE-SW (040 to 060°) trending structures are also identified.
74 hydrothermal chimney alignments were picked based on the topography they constitute over the sedimentary flats (Fig. 3). The two main alignment directions are ESE-WNW (090 to 120°) and ENE-WSW (060 to 090°) (Fig. 2c). Massive chimney structures of the GHCa south of the mapping area tends

https://doi.org/10.5194/egusphere-2023-397
Preprint. Discussion started: 14 March 2023

to be located at the intersection of these two alignment directions. N-trending alignments are also observed in the densest part in terms of chimneys (i.e. SHCa), but not in the southern part of the mapping area.

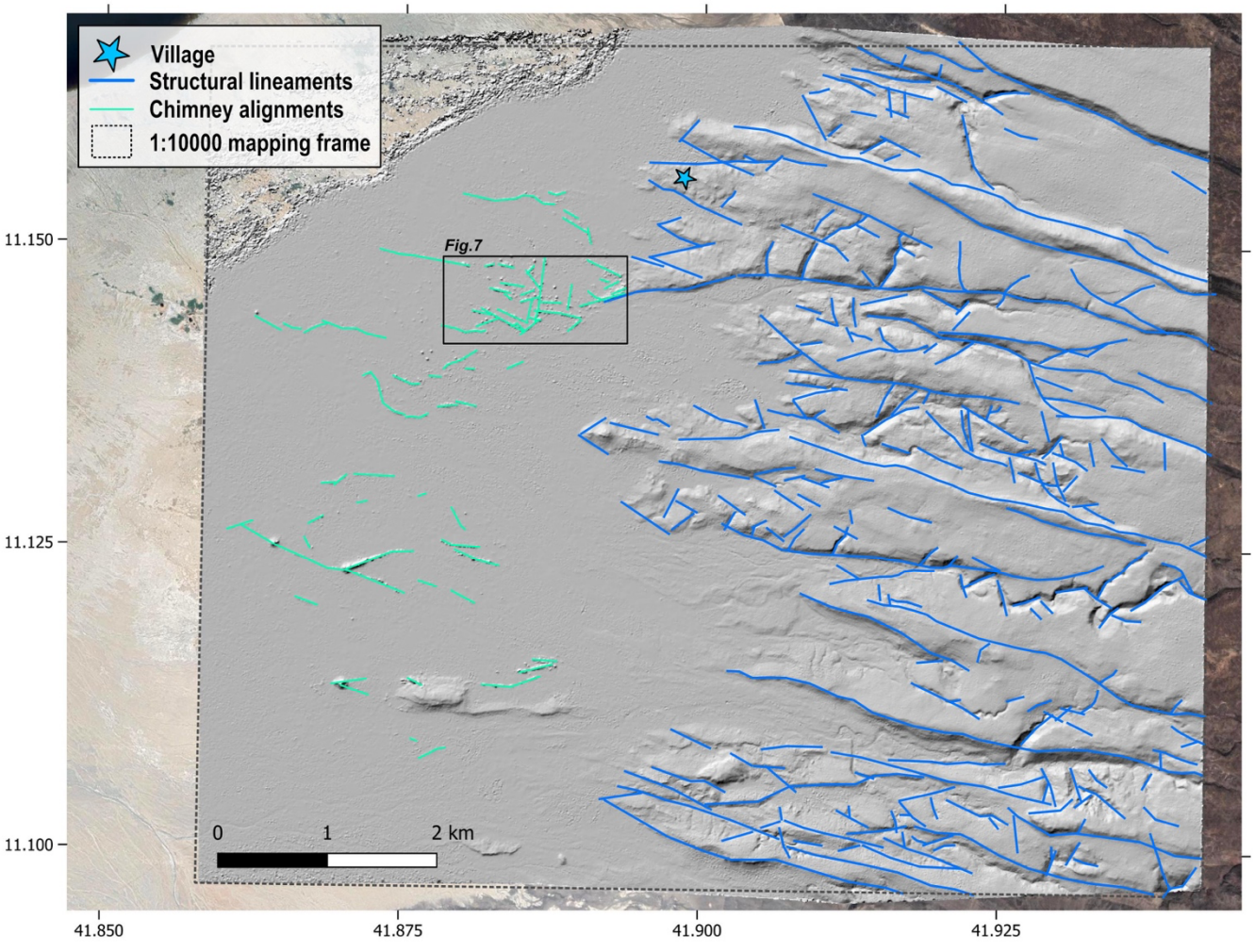

Figure 3: Lineament mapping of the LAGF area on a Pléiades dataset-based DEM hillshade image. Structural lineaments within the Stratoid Series hills are shown as blue lines. Hydrothermal chimney alignments observed over the basin sedimentary flats are shown as green lines. Map location is shown in Figure 1.

4.2 Structural geometry of the LAGF surrounding hills

Based on field observations and fault scarp morphology on satellite images, we added an interpretation of structural covering to the 1:60,000 scale lineament mapping results. This structural mapping is focused on a 40 km² area east to the LAGF. This densely faulted area displays variable topography that range from about 550 m (above sea level) in the east of the map to 240 m in the floor of the graben nearby the lake shore, with a general westward plunge of the Stratoid Series towards the basin (Fig. 4a).

https://doi.org/10.5194/egusphere-2023-397
Preprint. Discussion started: 14 March 2023

A significant number of ESE-trending lineaments produces scarps and topographic variations that can be attributed to normal faults. These normal faults can be further divided into two subsets along a north-south axis covering the area, as exhibited on topographic profiles (Fig. 4b). In the northern part of the area, both north- and south-dipping normal faults are observed, forming horst and graben structures with apparent fault throw at the surface up to a hundred meters and fault spacing of about 1 km (Fig. 5a). The southern part of the area exhibits mostly synthetic south-dipping normal faults, with a slightly denser fault spacing, that forms a tilted block geometry (Fig. 5b). Across this series of narrow horsts and grabens, overlapping synthetic normal faults interact and produce localized zones dipping steeper to the west, interpreted as relay ramps. The most prominent ramp is being identified in a graben of the northern part of the area (Fig. 5c). The dominant ESE-trending fault set is affected by a few N-trending structures, with no clear dip direction. These structures do not seem to crosscut faults, although some of these tend to be aligned, and rather seem to link 2 adjacent normal faults.

https://doi.org/10.5194/egusphere-2023-397
Preprint. Discussion started: 14 March 2023

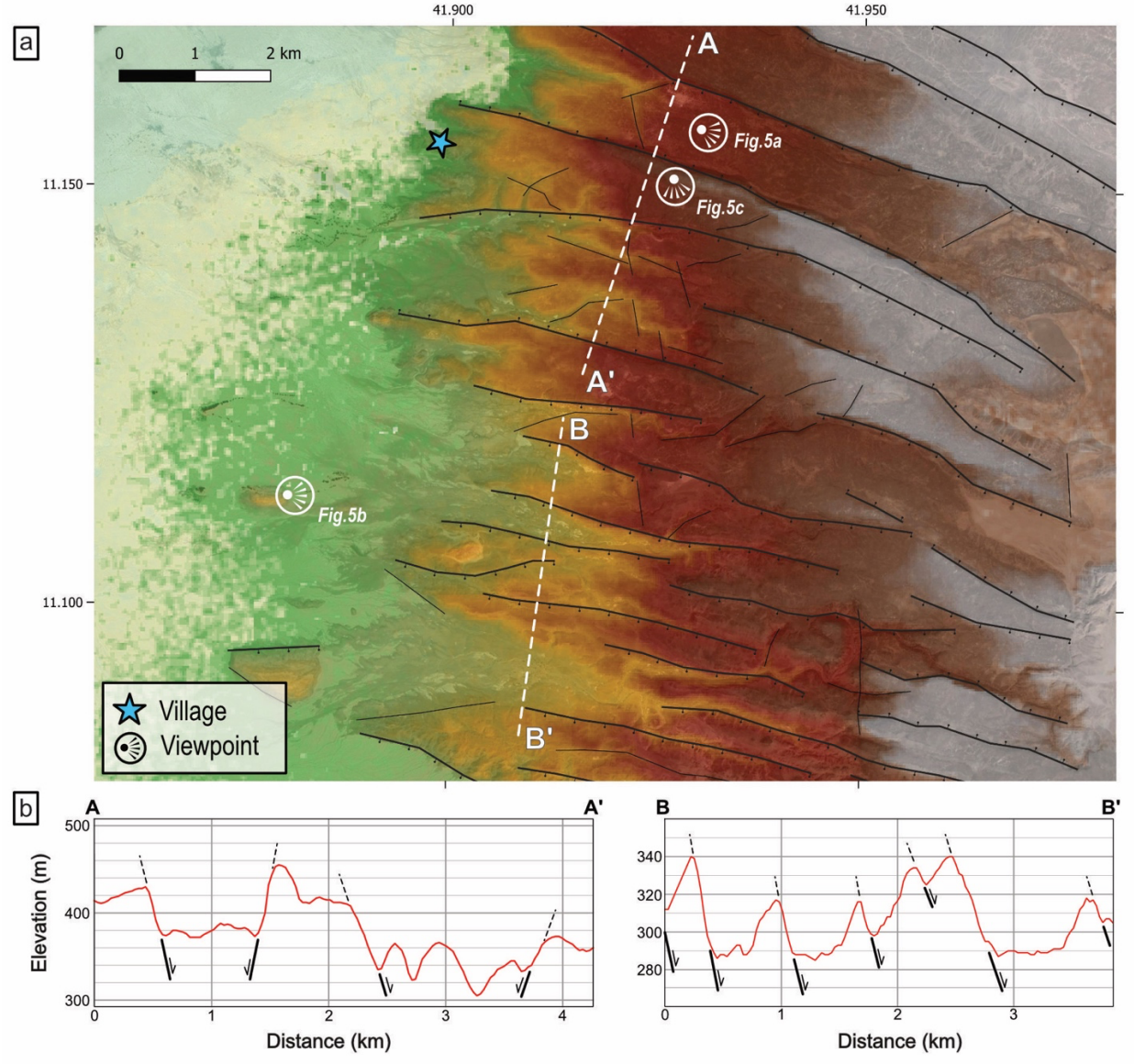

Figure 4: a) Topographic map of the LAGF area generated from SRTM Global DEM. Elevation ranges from ~240 m (pale green) to ~550 m (white). White dashed lines are locations of topographic profiles represented in Figure 4b. Normal faults, interpreted from field and topography observations, and unresolved lineaments from 1/60,000 scale structural lineament mapping are shown as black lines. Viewpoints location of Figure 5 is shown on the map. b) Topographic profiles extracted SRTM Global DEM, with uniform vertical exaggeration along the profiles. Normal faults location is pointed out on the profiles.

https://doi.org/10.5194/egusphere-2023-397
Preprint. Discussion started: 14 March 2023

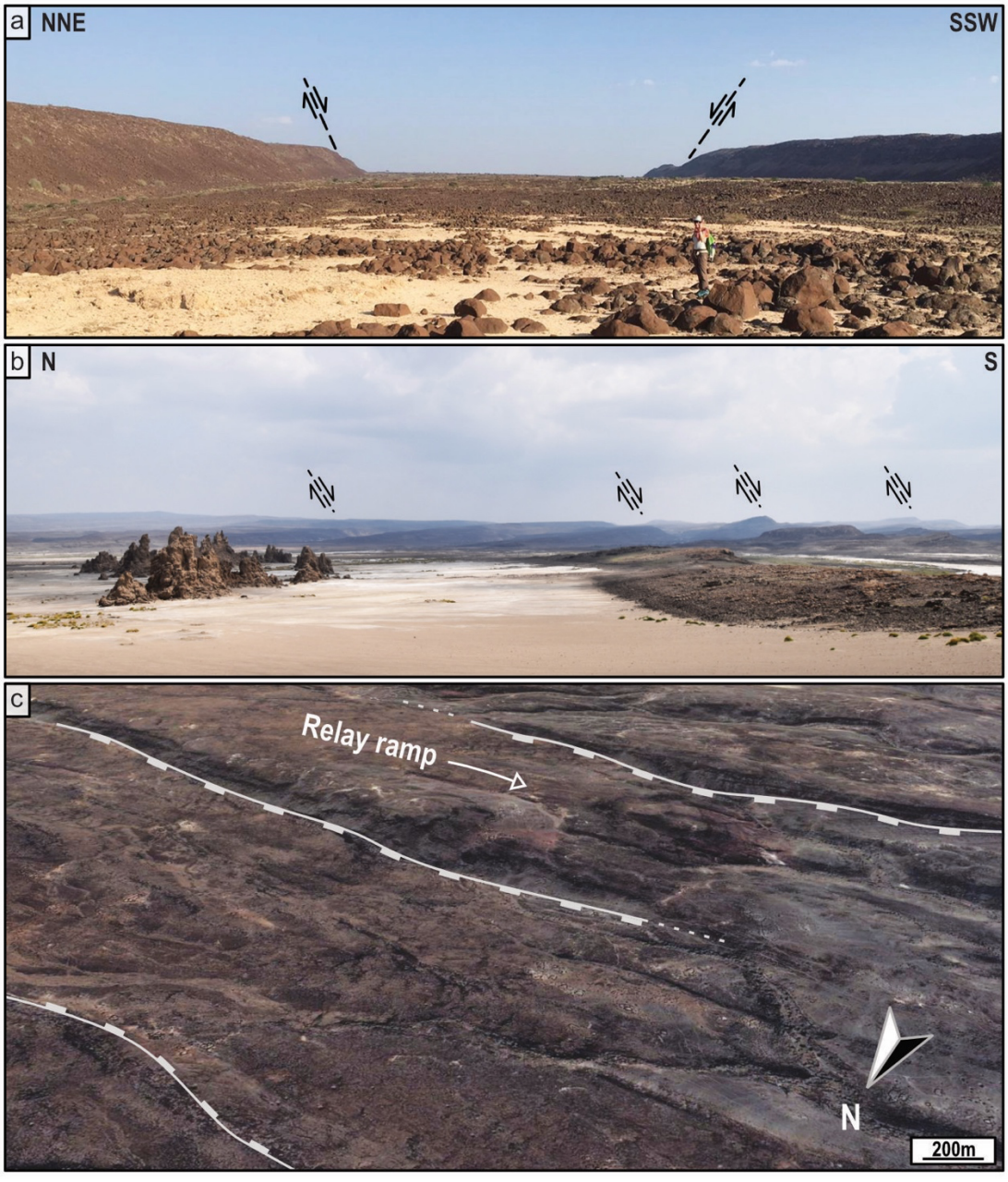

Figure 5: a) Graben geometry in the northern part of the LAGF area. b) Tilted blocks geometry in the southern part of the LAGF area. c) Perspective view of a relay ramp, generated from Google Earth (© Google Earth 2022). Location of these 3 viewpoints is represented on Figure 4.

4.3 Hydrothermal chimney fractures field analysis

Field observations of more than 100 hydrothermal chimneys located in the SHCa were carried out in order to support remote sensing data and images interpretation and investigate structural features within

https://doi.org/10.5194/egusphere-2023-397
Preprint. Discussion started: 14 March 2023

this chimney field. On the field, chimney alignments described above (Fig. 3) consist in the alignment of several individual and/or clustered structures. Such aligned structures can exhibit lateral continuity with the base of chimneys touching each other or can be separated (meter to decameter) with unconsolidated sediments (Fig. 6a, b). Numerous separated chimneys belonging to the same axis appear to be connected with inter-chimney materials consisting of localized spots of weakly-lithified carbonate and siliciclastic mixed materials outcropping on the surface according to the axis direction (Fig. 6c). Chimney clusters are generally elongated following the direction of the alignment they are connected to, with chimney summits lined up to the same direction (Fig. 6a). No relationship between macro-scale chimney morphology type and alignments was identified as different types were observed along the same alignment. No particular change in chimney size or morphology was recognized at the intersection of alignment axes.

Because of the high porosity and friability of chimney material, planar structures as fractures are difficult to be distinguished at the meso- and micro-scale within these features. In the field, macro-scale observations recognized two types of plurimetric long planar structures. The first type is composed of irregular cracks, generally sub-vertical with an aperture up to several centimeters. They were identified on many chimneys with no consistent azimuth direction between them (Fig. 6d). Such cracks, commonly propagating from the top to the base of the chimneys are considered as collapsing cracks with no tectonic origin. The second type are moderately to highly dipping (between 30 to 90°) plurimetric long planes that cut through the chimneys. A set of parallel planes or antithetic planes sharing the same azimuth is often found through the same chimney (Fig. 6b, e, f). 91 planes, identified through several tens of different chimney structures located in the SHCa, were measured in the field in order to analyze their orientation distribution (Fig. 7). No consistent relationship between planes orientation and chimney alignments direction was found in the field. These planes were either parallel or oblique to the alignment along which they were measured. The overall orientation distribution shows three dominant sets of N- (350 to 020°), ENE- (040 to 080°) and ESE- (090 to 120°) trending planes. The ESE-trending set is consistent to the ESE dominant structural direction observed in the LAGF area through structural lineaments and chimney alignments. The two other N- and ENE-trending sets of planes also show consistent directions to the chimney alignments, especially in this specific part of the SHCa that is the only one where N-S alignment were recognized. This orientation distribution, in addition to the morphology of these planar structures through the hydrothermal chimneys, suggests that these planes correspond to macro-scale tectonic fractures. A number of chimneys shaped by these fractures in their lower part exhibit a preserved bulbous form at their top (Fig. 6e, f). This morphology suggests these bulbous upper growths were formed after fracturing of the lower existing parts of the chimneys, the hydrothermal activity being maintained beyond. The formation of these chimneys is therefore considered as syn-tectonic.

https://doi.org/10.5194/egusphere-2023-397
Preprint. Discussion started: 14 March 2023

255 **Figure 6: Large-scale hydrothermal chimney distribution and characteristics. a) Drone aerial photograph of a part of the SHCa. b) Adjacent massive chimneys, exhibiting crosscutting subparallel planar structures with orientation. c) Sublinear weakly-lithified carbonate and siliciclastic mixed materials outcropping on the surface between hydrothermal chimneys. d) Irregular-shaped collapsing crack observed across a hydrothermal chimney. e) & f) Hydrothermal chimneys exhibiting bulbous-shaped tops bounded by crosscutting subparallel planar structures, with orientation.**

https://doi.org/10.5194/egusphere-2023-397
Preprint. Discussion started: 14 March 2023

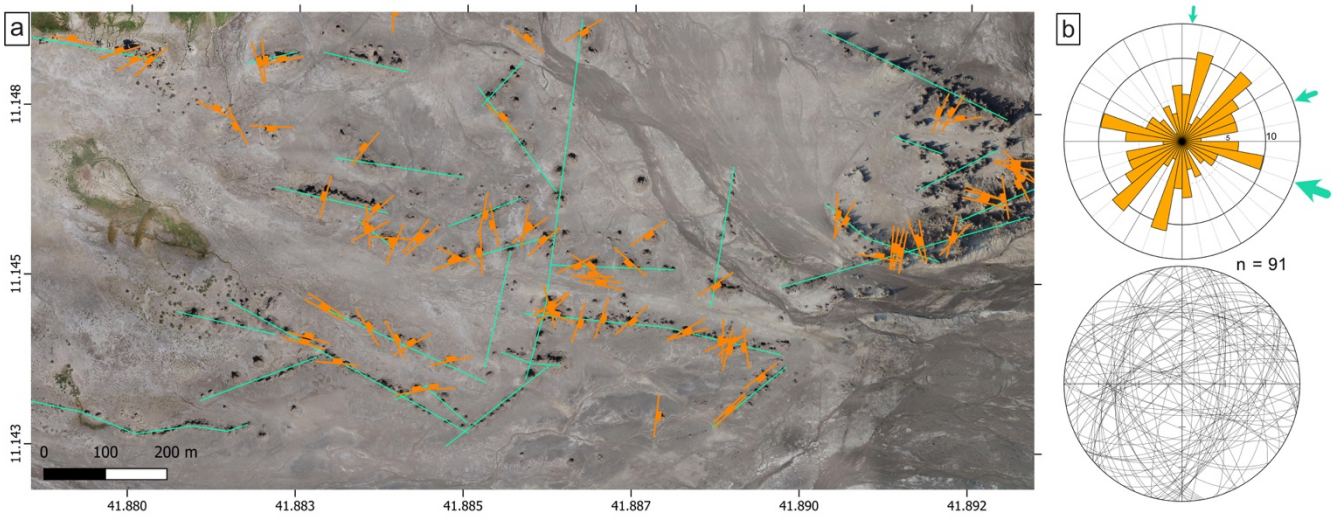

Figure 7: a) Location map of hydrothermal chimney crosscutting planar structures measured in the SHCa, represented as oriented orange symbols (satellite image from © Google Earth 2022). Green lines correspond to 1/10,000 scale hydrothermal chimney alignment mapped over the LAGF area. Map location is shown in Figure 3. b) Rose diagram and stereographic projection represent overall measurements of the hydrothermal chimney crosscutting planar structures. The different sized green arrows indicate the main directions of chimney alignments by relative importance (cf. Figure 2c).

4.4 Hot springs mapping

Hot springs represent another important hydrothermal feature of the LAGF. They generally form decimeter to meter-wide small ponds and flow towards the lake along small incisions through the sedimentary flats (Fig. 8a, b). These hot springs are commonly associated with active hydrothermal chimneys. They are found at their base and surround some of these chimneys, especially in the GHCa. However, many hot springs are also found in the LAGF area with no chimney in close proximity.
In comparison to the hyper-saline and highly alkaline (pH=9.86) waters of Lake Abhe, geothermal waters from these springs are moderately alkaline (pH=7.61–8.80) and fit for consumption for local wildlife (Awaleh et al., 2015). The continuous flow of these waters in this rather dry area allows the development of vegetation around these sources. This vegetation facilitates identification of the hot springs in the LAGF landscape as well as on the satellite images.
With the knowledge from field observations of several hot springs located in the SHCa and the GHCa, hot springs of the whole LAGF area were mapped using satellite images (Fig. 9). The majority of them are located in the northern part of the LAGF, with a distribution following the overall ESE-WNW structural trend. In this part of the LAGF, not all the hot springs are associated to hydrothermal chimneys, especially on the northern and western ends of the area where no such structures are observed near the sources. On the other hand, no hot springs were observed in the field or in the satellite images in the eastern part the SHCa, suggesting these hydrothermal chimneys to be currently inactive. Only chimneys from the northwestern part of the SHCa were observed with hot springs at their base. In the GHCa in the south, hot springs are associated with great chimneys of several tens of meters high. However, smaller sized chimneys in this area show no signs of geothermal water flow. A few springs

https://doi.org/10.5194/egusphere-2023-397
Preprint. Discussion started: 14 March 2023

were also identified at the contact of the Stratoid Series hills with the basin sediments where structural lineaments were mapped.

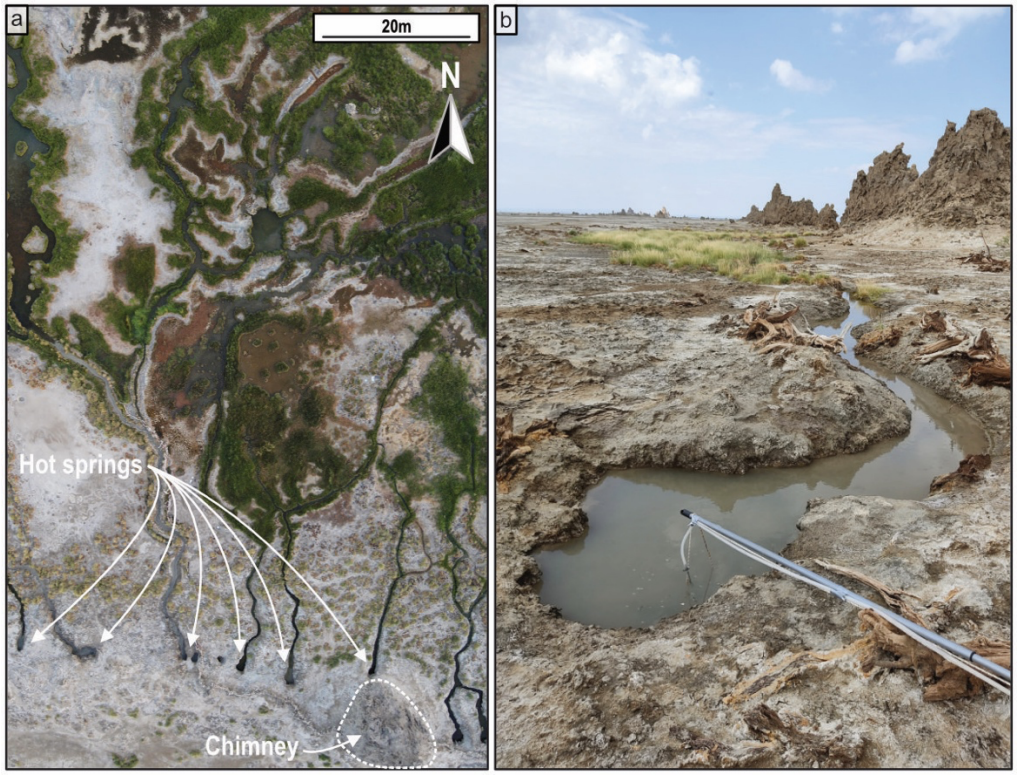

290 **Figure 8: a) Drone aerial photograph showing aligned hot springs observed in the SHCa, flowing northward with associated vegetation. b) Example of a hot spring found in the sedimentary flats of the LAGF area (geochemistry sampling device for scale).**

https://doi.org/10.5194/egusphere-2023-397
Preprint. Discussion started: 14 March 2023

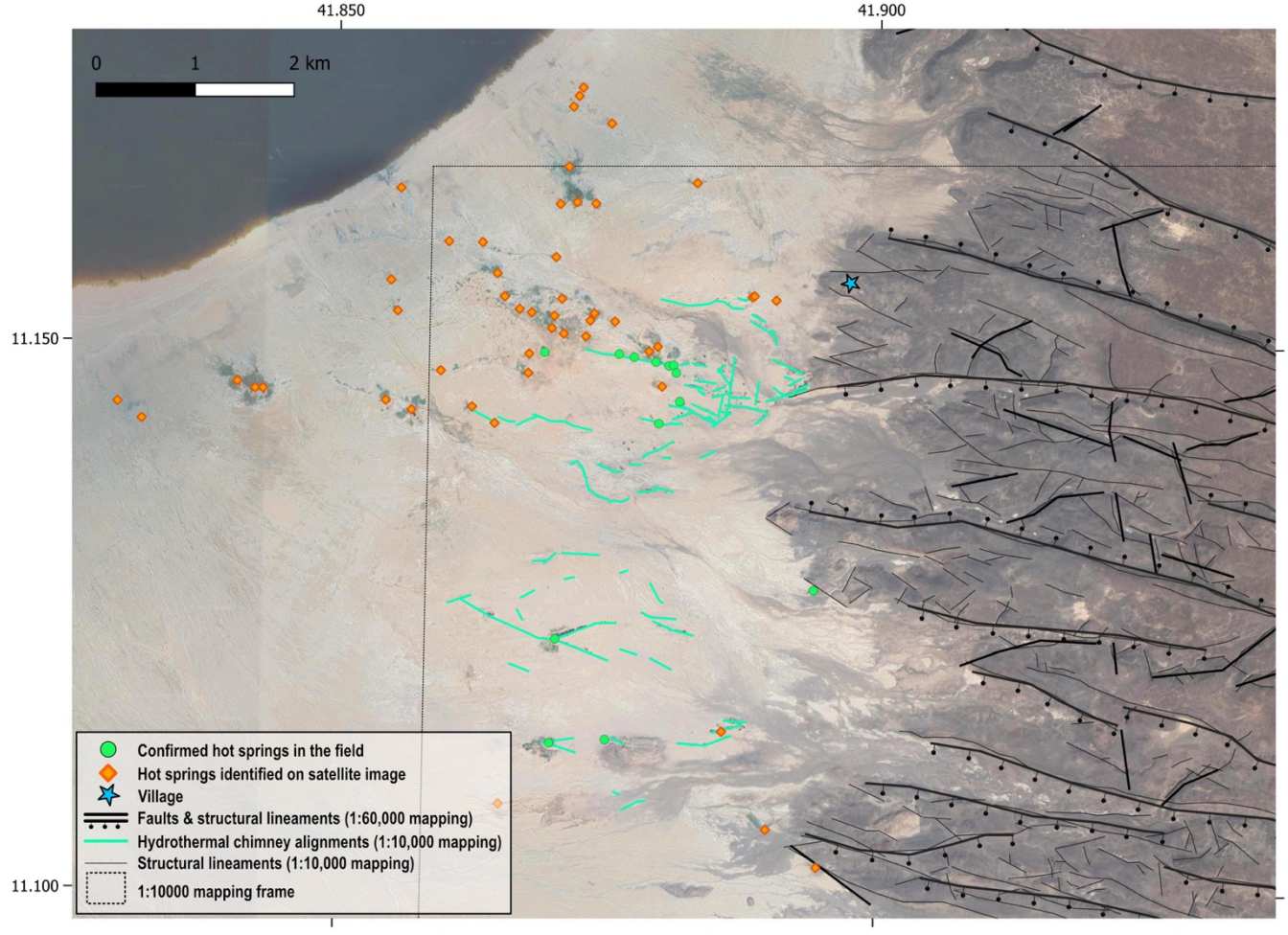

Figure 9: Location map of hot springs in the LAGF area, with structural lineament mapping results (satellite image from © Google Earth 2022).

5 Discussion

5.1 Structural features of the LAGF

Structural features of the LAGF area are dominated by ESE-trending extensional faults that form a series of narrow elongated horst, graben and half-graben structures visible east of the LAGF in the Stratoid Series. This structural pattern is recognizable over a wide area, tens of kilometers north through the northern Gob Aad graben shoulder, up to the southwest boundary with the adjacent Hanle graben (Tesfaye et al., 2008). Considering the general length of several kilometers to tens of kilometers of these structures, faults directly visible east of the LAGF are likely to propagate westward within the volcanic series buried underneath the basin and the geothermal active area. Satellite images and field investigations indicate an evolution in the dip of these ESE-trending faults between those observed in

https://doi.org/10.5194/egusphere-2023-397
Preprint. Discussion started: 14 March 2023

the northern and the southern parts through the Stratoid Series east to the LAGF. A set of synthetic and antithetic normal faults, forming horst and graben structures, is observed in the northern part while a denser network of south-dipping synthetic faults associated to tilted blocks is observed in the southern part. A possible explanation for such geometry evolution is that the extension rate was higher north closer to the Gob Aad graben north boundary faults. With respect to this bimodal fault geometry, hydrothermal manifestations are found more numerous in the northern part of the LAGF in the continuation of the horst and graben structures.

Accommodation zones between adjacent normal faults with complex arrays of smaller-scale structures and with at least one significant relay ramp are recognized nearby the LAGF. The latter structure type is marked in the area by significant topographic variations (Fig. 5c). Relay zones were extensively documented in continental rift systems to result in the interaction between adjacent and/or overlapping fault segments, by accommodating displacement transfer through complex deformation structures (e.g. Trudgill and Cartwright, 1994; Peacock, 2002; Hemelsdaël and Ford, 2016). Variety of typical accommodation zone structures were described north to the LAGF and the Gob Aad graben, in the Dobe and Hanle grabens, including ramp development, normal faulting of the ramp, complex block rotation and development of breaching faults that link the interacting graben-bounding faults (Tesfaye et al., 2008). As displacement increases, ramps steepen and become broken up by crosscutting faults developed near the hinge zones and form elongate fault blocks that can rotate along antithetic faults. These breaching faults are considered in part as open (mode 1) fractures. With relay ramps identified in the LAGF surrounding hills, the minor sets of N- and NWN-trending structural lineaments are interpreted, at least in some cases, as breaching faults. These structures indeed exhibit similar shape and characteristics to the breaching faults described in the Dole and Hanle grabens located about 50/60 km north, oblique to the dominant ESE-trending extensional faults. No block rotation is however recognized in the LAGF area. This can be due to the fact that these breaching faults that precede rotation are not sufficiently developed to separate in depth fault blocks from the ramp (i.e. the hanging wall).

A significant number of these N-trending breaching faults tends to be aligned (Fig. 4). With a significant extension rate and displacement transfer, crosscutting breaching faults are described to link together, forming a continuous fault connecting originally separated fault segments (Tesfaye et al., 2008; Fossen and Rotevatn, 2016). With such an alignment instead of a commonly described en-echelon distribution, the development of these breaching faults may be influenced by preexisting structures underlying the Stratoid Series that control in part the segmentation of this extensional fault system (e.g. Morley et al., 2004; Tong et al., 2014; Whipp et al., 2014). Such breaching fault linkage could contribute to explain the overall N-trending boundary between the Stratoid Series hills and the basin sediments of the LAGF area, as well as the fault-controlled depression filled with sediments that is observed about 10 km east from the LAGF within the volcanic series (Fig. 1, 9). This assumption of a significant influence of N-trending structures on this area's morphology can be supported by multi-methods geophysics surveys carried out in the LAGF. Resistivity model indicates a low resistivity layer, approximately 300-400 m thick in the SHCa and GHCa vicinity, interpreted as the thickness of conductive sediments (Fahman et al., 2018). In comparison to the slight dip of the Stratoid Series hills plunging westward within the basin, the thickness of these sediments may appear relatively important. This may suggest the existence of such N-trending extensional structures that favor the Stratoid Series

https://doi.org/10.5194/egusphere-2023-397
Preprint. Discussion started: 14 March 2023

burial. In addition to the main ESE-trending normal faults, ramps and associated breaching faults may as well be buried and masked by the sedimentary cover.

5.2 Hydrothermal surface manifestations distribution and evolution

In geothermal areas, hydrothermal manifestations such as thermal springs and travertine depositions have been often associated with active faulting and tectonics (Bense et al., 2013; Frery et al., 2015; Brogi et al., 2021). The concept of "travitonics", introduced by Hancock et al. (1999) describes the inseparable processes between brittle deformation at shallow crustal levels and travertine deposition. Among the different travertine deposit types (i.e. fissure ridge- vs. chimney-type deposits) produced from hydrothermal fluids discharged from thermal springs, many studies have reinforced the evidences of travertine deposition along the traces of brittle structures (De Filippis et al., 2013; Brogi et al., 2021, and references therein). The distribution of the LAGF hydrothermal manifestations following these structural orientations described in the area support the idea of tectonically driven morpho-tectonic features.

LAGF hydrothermal chimneys correspond to mound-type deposits, which are end-members in comparison to fissure-ridge deposits (i.e. continuous massive travertine over fault trace). Fissure-ridge development is inhibited by faults affecting unconsolidated sediments. In such case, fault-related permeability is described as strongly compartmentalized and fluids emerge only in isolated spots along the fault trace (Brogi et al., 2021). Among several parameters (hydrothermal fluid and CO_2 fluxes, lake water level, etc.), fault and fracture-induced permeability controls chimneys localization and development. This permeability can be enhanced at structural intersections, marked by hints of enhanced hydrothermal activity (e.g. chimney size, density). Structural intersections with "x-shaped" fault and fracture networks can indeed act as dilatational zones and fluid preferential pathways under various tectonic stress regimes, producing significant relative vertical fracture permeability (e.g. Sibson, 1996, 2000; Person et al., 2012). In the GHCa, the massive and currently active chimneys are distributed at the intersection between ESE- and ENE-trending hydrothermal traces (Fig. 3). In the SHCa, intersecting patterns localizing higher hydrothermal activity are more complex to observe as this area has an overall higher chimney density. This density may reflect a more diffused hydrothermal fluid flow thanks to the numerous intersecting structural traces (ESE-, ENE-, NNE-trending), underlined by the chimney alignments that composed this area. Chimney distribution over these 2 areas therefore suggests that fault and fracture-induced permeability in the LAGF is favored locally by structural intersections.

Hydrothermal chimney and travertine deposition testify of the high encrusting capacity of hydrothermal fluids along the conduits (Brogi et al., 2021). Long-lived hydrothermal flow and renewed fault and fracture-induced permeability is guaranteed by tectonic activity (Curewitz and Karson, 1997). Active faulting and fracturing enable continual re-opening of fluid flow conduits despite potential clogging of fractures due to mineral precipitation. Age of the LAGF chimneys is poorly constrained. These structures, formed subaqueously during the successive lake level rises of the Lake Abhe throughout the Late Pleistocene and Holocene, have been deposited sequentially over multiple cycles of lake transgression and regression (DeMott et al., 2021). The current hot springs, as well as the different phases of hydrothermal chimney formation of the LAGF therefore indicate this area to have undergone

https://doi.org/10.5194/egusphere-2023-397
Preprint. Discussion started: 14 March 2023

regular tectonic pulses over the last few tens of thousands of years, renewing fracture permeability and triggering (re-)activation of thermal springs. Macro-scale syn-tectonic fractures that shaped some of the chimneys' morphology during their formation over time in the SHCa support this idea (Fig. 6e, f). The SHCa exhibits in its eastern part a significant number of inactive hydrothermal chimneys (i.e. no steam vent or springs). On the other hand, many hot springs with no associated chimney features are recognized in the northern and western part of the SHCa. The relative current lowstand lake level can explain the absence of chimneys formed alongside recent hotsprings. Therefore, the lack of current hydrothermal manifestations within extinguished chimneys in the east, as well as the recent springs in the north and west may suggest a westward progressive lateral evolution of the hydrothermal fluid outflows over time. Given the sequential depositional model of the chimneys during successive transgressive intervals described by DeMott et al. (2021), some chimneys are likely to have been buried during a transgressive interval if they weren't active at this moment. Offshore seismic reflection data show such inactive chimneys buried in the northern part of the lake (DeMott et al., 2021). Other buried chimneys are therefore likely to be present in the LAGF area, depending on the lateral evolution of the fluid outflows over time. Consequently, continuous tectonic activity over at least tens of thousands of years maintained an overall sufficient permeability to develop these remarkable hydrothermal surface manifestations all over the LAGF area. However, spatial outflow evolution appears to have occurred depending on localized tectonic pulses, fracturing and thermal springs (re-)activation.

5.3 Implications for the LAGF development

The structural analysis of the LAGF surrounding hills and the distribution of hydrothermal manifestations indicate the presence in the area of fault interaction and accommodation zones, as relay ramps and fault intersections, generally described as favorable pathways for fluid flow. Relay ramps, breached or not, typically exhibit increased structural complexity compared to a single fault zone, with enhanced density and connectivity of faults and fractures and a wider range of orientations (e.g. Peacock and Sanderson, 1994; Peacock, 2002; Conneally et al., 2014). These characteristics make relay ramps a prime pathway for vertical fluid flow in the crust, affecting all kinds of fluids (e.g. hydrothermal, CO2, hydrocarbons, etc.) (Fossen & Rotevatn, 2016, and references therein). Similarly, intersection of multiple faults represents a high structural complexity zone that can act as fluid preferential pathway with significant vertical fracture permeability, especially in low-porosity rocks (Curewitz & Karson, 1997; Sibson, 2000). Structural intersections are described as well as key features for outflow and exploitation of different kinds of fluids (e.g. Gartrell et al., 2004; Walter et al., 2019). More specifically regarding geothermal systems, outflows occurring predominantly at fault intersections have been extensively described for fault-controlled plays (e.g. Craw, 2000; Rowland and Sibson, 2004; Taillefer et al., 2017). An inventory of more than 400 geothermal actives sites in the Great Basin region (USA) highlighted that more than half of these sites are hosted by fault interaction zones, as fault intersections and relay ramps (Faulds et al., 2011). These latter structural features therefore appear as reliable prime targets for the LAGF development.

The hydrothermal chimneys described in this area represent a useful surface proxy to decipher key structural features distribution in depth and help identifying of the current most active upflow zones. Complementary geophysics surveys would however be needed to confirm this and to precise potential

https://doi.org/10.5194/egusphere-2023-397
Preprint. Discussion started: 14 March 2023

drilling targets. Awaleh et al. (2015) indicated that the LAGF reservoir is fed by meteoric water that penetrates downwards through the fracture network in the basalt Stratoid Series and combine with deep regional groundwater in the thermal aquifer to a maximum depth of about 1 km. Numerous unresolved questions remain about the geothermal reservoir parameters (depth, extent, host rock nature, etc.), the transition and localized flow processes from basalt series to poorly consolidated sediments, or the LAGF specific location in the Gob Aad basin. The LAGF appears indeed as the only significant geothermal occurrence for exploitation in the entire basin. These unraveled parameters therefore represent critical information to start geothermal development in this area.

6 Conclusion

The LAGF Stratoid Series surrounding hills, as well as the hydrothermal surface manifestations of this area, were characterized through a multiscale structural survey and a lineament distribution mapping. Structural features of the LAGF area are dominated by ESE-trending extensional faults. The overall geometry of the structural blocks delimited by these faults evolves between the north and the south of the studied area. Synthetic and antithetic faults form a series of narrow elongated horsts and grabens in the northern part whereas a denser network of south-dipping synthetic faults form half-grabens associated with tilted blocks in the southern part. Accommodation zones between adjacent normal faults, with at least one significant relay ramp were also identified in this studied area. Some of the structural lineaments identified with a N- and NWN trend may represent possible breaching faults of such accommodation features. The hydrothermal surface manifestations mapping reveals the control of structural directions on chimneys and hot springs distribution, following the main lineament trends. Hints of higher hydrothermal activity localized at intersecting structural traces are also observed. Hydrothermal chimneys represent proxies of the LAGF structural features distribution in depth and therefore suggest that structural intersections can locally enhance fault and fracture-induced permeability. Plurimetric long tectonic fractures that cut through the hydrothermal chimneys were also recognized, orientation distribution being consistent with chimney alignment directions and the main structural trends of the area. Field observations, in conjunction with satellite images analysis, suggested a progressive lateral evolution of the LAGF hydrothermal fluid outflows over time, with regular tectonic pulses renewing fracture permeability through chimneys and triggering (re-)activation of thermal springs. This study finally demonstrates the strong connection between LAGF structural features and the hydrothermal manifestations distribution. It provides new insights on the local tectonically driven fluid flow evolution. This work may therefore support further exploration of this remarkable site and promote geothermal development in the area.

7 Data availability

All raw data can be provided by the corresponding authors upon request.

https://doi.org/10.5194/egusphere-2023-397
Preprint. Discussion started: 14 March 2023

8 Author contributions

YG acquired the funding; all authors contributed to collect data and conceptualize the study; BW wrote the manuscript draft and produced the figures; YG, AF, NC and MD reviewed and edited the manuscript.

9 Competing interests

The authors declare that they have no known competing financial interests or personal relationships that could have appeared to influence the work reported in this paper.

10 Acknowledgments

This study was carried out within the framework of the "Geothermal Village" program under the LEAP-RE partnership, all the partners are gratefully acknowledged. We are greatly thankful to Jacques Varet and ODDEG partners for field insights and logistical support during fieldwork. We are grateful to Jérôme Ammann for providing drone photographs, and Carolina Dantas Cardoso for providing hot spring photographs used in this paper. We thank the reviewers and the journal editor for their thoughtful and thorough review and editorial suggestions. We also greatly acknowledge Déborah Jaeger for read-proofing.

11 Financial support

This work benefited from the financial support from the European Commission Horizon 2020 funded project LEAP-RE (Long-Term Joint EU-AU Research and Innovation Partnership on Renewable Energy), registered under the grant agreement ID 963530 (DOI:10.3030/963530).

12 References

Abdillahi, O., Mohamed, A., Moussa, K., and Khaireh, A.: Geothermal development in Republic of Djibouti: a country update report, in: Proceedings of the 6th African Rift Geothermal Conference, Addis Ababa, Ethiopia, 16, 2016.

ARGeo: 9th African Rift Geothermal Conference (ARGEO-C9) Report, Djibouti, 2022.

Awaleh, M. O., Hoch, F. B., Boschetti, T., Soubaneh, Y. D., Egueh, N. M., Elmi, S. A., Mohamed, J., and Khaireh, M. A.: The geothermal resources of the Republic of Djibouti — II: Geochemical study of the Lake Abhe geothermal field, Journal of Geochemical Exploration, 159, 129–147, https://doi.org/10.1016/j.gexplo.2015.08.011, 2015.

Awaleh, M. O., Boschetti, T., Soubaneh, Y. D., Kim, Y., Baudron, P., Kawalieh, A. D., Ahmed, M. M., Daoud, M. A., Dabar, O. A., Kadieh, I. H., Adiyaman, Ö., Elmi, S. A., and Chirdon, M. A.:

https://doi.org/10.5194/egusphere-2023-397
Preprint. Discussion started: 14 March 2023

Geochemical, multi-isotopic studies and geothermal potential evaluation of the complex Djibouti volcanic aquifer (republic of Djibouti), Applied Geochemistry, 97, 301–321, https://doi.org/10.1016/j.apgeochem.2018.07.019, 2018.

Bense, V. F., Gleeson, T., Loveless, S. E., Bour, O., and Scibek, J.: Fault zone hydrogeology, Earth-Science Reviews, 127, 171–192, https://doi.org/10.1016/j.earscirev.2013.09.008, 2013.

Beyene, A. and Abdelsalam, M. G.: Tectonics of the Afar Depression: A review and synthesis, Journal of African Earth Sciences, 41, 41–59, https://doi.org/10.1016/j.jafrearsci.2005.03.003, 2005.

Brogi, A., Capezzuoli, E., Karabacak, V., Alcicek, M. C., and Luo, L.: Fissure Ridges: A Reappraisal of Faulting and Travertine Deposition (Travitonics), Geosciences, 11, 278, https://doi.org/10.3390/geosciences11070278, 2021.

Chorowicz, J.: The East African rift system, Journal of African Earth Sciences, 43, 379–410, https://doi.org/10.1016/j.jafrearsci.2005.07.019, 2005.

Conneally, J., Childs, C., and Walsh, J. J.: Contrasting origins of breached relay zone geometries, Journal of Structural Geology, 58, 59–68, https://doi.org/10.1016/j.jsg.2013.10.010, 2014.

Craw, D.: Fluid flow at fault intersections in an active oblique collision zone, Southern Alps, New Zealand, Journal of Geochemical Exploration, 69–70, 523–526, https://doi.org/10.1016/S0375-6742(00)00094-7, 2000.

Curewitz, D. and Karson, J. A.: Structural settings of hydrothermal outflow: Fracture permeability maintained by fault propagation and interaction, Journal of Volcanology and Geothermal Research, 79, 149–168, https://doi.org/10.1016/S0377-0273(97)00027-9, 1997.

D'Amore, F., Giusti, D., and Abdallah, A.: Geochemistry of the high-salinity geothermal field of Asal, Republic of Djibouti, Africa, Geothermics, 27, 197–210, https://doi.org/10.1016/S0375-6505(97)10009-8, 1998.

De Filippis, L., Faccenna, C., Billi, A., Anzalone, E., Brilli, M., Soligo, M., and Tuccimei, P.: Plateau versus fissure ridge travertines from Quaternary geothermal springs of Italy and Turkey: Interactions and feedbacks between fluid discharge, paleoclimate, and tectonics, Earth-Science Reviews, 123, 35–52, https://doi.org/10.1016/j.earscirev.2013.04.004, 2013.

Dekov, V. M., Egueh, N. M., Kamenov, G. D., Bayon, G., Lalonde, S. V., Schmidt, M., Liebetrau, V., Munnik, F., Fouquet, Y., Tanimizu, M., Awaleh, M. O., Guirreh, I., and Le Gall, B.: Hydrothermal carbonate chimneys from a continental rift (Afar Rift): Mineralogy, geochemistry, and mode of formation, Chemical Geology, 387, 87–100, https://doi.org/10.1016/j.chemgeo.2014.08.019, 2014.

Demange, J., Di Paola, G., Lavigne, J., Lopoukhine, M., and Stieltjes, L.: Etude géothermique du Territoire Français des Afars et des Issas, avril 1971, Paris, Rapport BRGM, 1971.

DeMott, L. M., Scholz, C. A., and Awaleh, M. O.: Lacustrine carbonate towers of Lake Abhe, Djibouti: Interplay of hydrologic and microbial processes, Sedimentary Geology, 424, 105983, https://doi.org/10.1016/j.sedgeo.2021.105983, 2021.

Deniel, C., Vidal, P., Coulon, C., Vellutini, P.-J., and Piguet, P.: Temporal evolution of mantle sources during continental rifting: The volcanism of Djibouti (Afar), J. Geophys. Res., 99, 2853–2869, https://doi.org/10.1029/93JB02576, 1994.

Fahman, H. A., Salahadine, M., and Haissama, O.: Geophysical study on Lake Abhe geothermal prospect, Djibouti, in: Proceedings of the 7th African Rift Geothermal Conference, Kigali, Rwanda, 14, 2018.

https://doi.org/10.5194/egusphere-2023-397
Preprint. Discussion started: 14 March 2023

Faulds, J. E., Hinz, N. H., Coolbaugh, M. F., Cashman, P. H., Kratt, C., Dering, G., Edwards, J., Mayhew, B., and McLachlan, H.: Assessment of Favorable Structural Settings of Geothermal Systems in the Great Basin, Western USA, in: GRC Transactions, San Diego, CA, 777–783, 2011.

Fossen, H. and Rotevatn, A.: Fault linkage and relay structures in extensional settings—A review, Earth-Science Reviews, 154, 14–28, https://doi.org/10.1016/j.earscirev.2015.11.014, 2016.

Frery, E., Gratier, J.-P., Ellouz-Zimmerman, N., Loiselet, C., Braun, J., Deschamps, P., Blamart, D., Hamelin, B., and Swennen, R.: Evolution of fault permeability during episodic fluid circulation: Evidence for the effects of fluid–rock interactions from travertine studies (Utah–USA), Tectonophysics, 651–652, 121–137, https://doi.org/10.1016/j.tecto.2015.03.018, 2015.

Gall, B. L., Maury, R. C., and Jalludin, M.: Géologie de Djibouti: notice de la carte géologique au 1:200000 de la République de Djibouti, Édition CERD, 2018.

Gartrell, A., Zhang, Y., Lisk, M., and Dewhurst, D.: Fault intersections as critical hydrocarbon leakage zones: integrated field study and numerical modelling of an example from the Timor Sea, Australia, Marine and Petroleum Geology, 21, 1165–1179, https://doi.org/10.1016/j.marpetgeo.2004.08.001, 2004.

Gasse, E. and Street, F. A.: Late Quaternary Lake-level fluctuations and environments of the northern Rift valley and Afar region (Ethiopia and Djibouti), Palaeogeography, Palaeoclimatology, Palaeoecology, 24, 279–325, https://doi.org/10.1016/0031-0182(78)90011-1, 1978.

Gasse, F.: Evolution of Lake Abhe (Ethiopia and TFAI), from 70,000 b.p., Nature, 265, 42–45, https://doi.org/10.1038/265042a0, 1977.

Hancock, P. L., Chalmers, R. M. L., Altunel, E., and Çakir, Z.: Travitonics: using travertines in active fault studies, Journal of Structural Geology, 21, 903–916, https://doi.org/10.1016/S0191-8141(99)00061-9, 1999.

Hemelsdaël, R. and Ford, M.: Relay zone evolution: a history of repeated fault propagation and linkage, central Corinth rift, Greece, Basin Res, 28, 34–56, https://doi.org/10.1111/bre.12101, 2016.

Houssein, B., Chandrasekharam, D., Chandrasekhar, V., and Jalludin, M.: Geochemistry of thermal springs around Lake Abhe, Western Djibouti, International Journal of Sustainable Energy, 33, 1090–1102, https://doi.org/10.1080/14786451.2013.813027, 2013.

Houssein, D. E. and Axelsson, G.: Geothermal resources in the Asal Region, Republic of Djibouti: An update with emphasis on reservoir engineering studies, Geothermics, 39, 220–227, https://doi.org/10.1016/j.geothermics.2010.06.006, 2010.

Huttrer, G. W.: Geothermal Power Generation in the World 2015-2020 Update Report, in: Proceedings World Geothermal Congress 2020+1, Reykjavik, Iceland, 17, 2021.

IRENA: Geothermal Development in Eastern Africa: Recommendations for power and direct use, International Renewable Energy Agency, Abu Dhabi, 2020.

Jolie, E., Scott, S., Faulds, J., Chambefort, I., Axelsson, G., Gutiérrez-Negrín, L. C., Regenspurg, S., Ziegler, M., Ayling, B., Richter, A., and Zemedkun, M. T.: Geological controls on geothermal resources for power generation, Nat Rev Earth Environ, 2, 324–339, https://doi.org/10.1038/s43017-021-00154-y, 2021.

Khalidi, L., Mologni, C., Ménard, C., Coudert, L., Gabriele, M., Davtian, G., Cauliez, J., Lesur, J., Bruxelles, L., Chesnaux, L., Redae, B. E., Hainsworth, E., Doubre, C., Revel, M., Schuster, M., and Zazzo, A.: 9000 years of human lakeside adaptation in the Ethiopian Afar: Fisher-foragers and the first

https://doi.org/10.5194/egusphere-2023-397
Preprint. Discussion started: 14 March 2023

pastoralists in the Lake Abhe basin during the African Humid Period, Quaternary Science Reviews, 243, 106459, https://doi.org/10.1016/j.quascirev.2020.106459, 2020.
Michon, L., Famin, V., and Quidelleur, X.: Evolution of the East African Rift System from trap-scale to plate-scale rifting, Earth-Science Reviews, 231, 104089, https://doi.org/10.1016/j.earscirev.2022.104089, 2022.
Moeck, I. S.: Catalog of geothermal play types based on geologic controls, Renewable and Sustainable Energy Reviews, 37, 867–882, https://doi.org/10.1016/j.rser.2014.05.032, 2014.
Morley, C. K., Haranya, C., Phoosongsee, W., Pongwapee, S., Kornsawan, A., and Wonganan, N.: Activation of rift oblique and rift parallel pre-existing fabrics during extension and their effect on deformation style: examples from the rifts of Thailand, Journal of Structural Geology, 26, 1803–1829, https://doi.org/10.1016/j.jsg.2004.02.014, 2004.
Moussa, O. A. and Souleiman, H.: Country Report, Geothermal Development in Djibouti Republic, in: Proceedings World Geothermal Congress 2015, Melbourne, Australia, 5, 2015.
NASA JPL: NASA Shuttle Radar Topography Mission Global 1 arc second, https://doi.org/10.5067/MEASURES/SRTM/SRTMGL1.003, 2013.
Peacock, D. C. and Sanderson, D. J.: Geometry and development of relay ramps in normal fault systems, AAPG bulletin, 78, 147–165, 1994.
Peacock, D. C. P.: Propagation, interaction and linkage in normal fault systems, Earth-Science Reviews, 58, 121–142, https://doi.org/10.1016/S0012-8252(01)00085-X, 2002.
Person, M., Hofstra, A., Sweetkind, D., Stone, W., Cohen, D., Gable, C. W., and Banerjee, A.: Analytical and numerical models of hydrothermal fluid flow at fault intersections: Fluid flow at fault intersections, Geofluids, 12, 312–326, https://doi.org/10.1111/gfl.12002, 2012.
Polun, S. G., Gomez, F., and Tesfaye, S.: Scaling properties of normal faults in the central Afar, Ethiopia and Djibouti: Implications for strain partitioning during the final stages of continental breakup, Journal of Structural Geology, 115, 178–189, https://doi.org/10.1016/j.jsg.2018.07.018, 2018.
Rowland, J. V. and Sibson, R. H.: Structural controls on hydrothermal flow in a segmented rift system, Taupo Volcanic Zone, New Zealand, Geofluids, 4, 259–283, https://doi.org/10.1111/j.1468-8123.2004.00091.x, 2004.
Rubio-Maya, C., Ambríz Díaz, V. M., Pastor Martínez, E., and Belman-Flores, J. M.: Cascade utilization of low and medium enthalpy geothermal resources − A review, Renewable and Sustainable Energy Reviews, 52, 689–716, https://doi.org/10.1016/j.rser.2015.07.162, 2015.
Samod, Y. H., Samatar, A. M., and Hassan, M. M.: Geological study of Lake Abhe, geothermal field, in: Proceedings of the 7th African Rift Geothermal Conference, Kigali, Rwanda, 8, 2018.
Sibson, R. H.: Structural permeability of fluid-driven fault-fracture meshes, Journal of Structural Geology, 18, 1031–1042, https://doi.org/10.1016/0191-8141(96)00032-6, 1996.
Sibson, R. H.: Fluid involvement in normal faulting, Journal of Geodynamics, 29, 469–499, https://doi.org/10.1016/S0264-3707(99)00042-3, 2000.
Stober, I. and Bucher, K.: Geothermal Energy: From Theoretical Models to Exploration and Development, Springer International Publishing, Cham, https://doi.org/10.1007/978-3-030-71685-1, 2021.

https://doi.org/10.5194/egusphere-2023-397
Preprint. Discussion started: 14 March 2023

Taillefer, A., Soliva, R., Guillou-Frottier, L., Le Goff, E., Martin, G., and Seranne, M.: Fault-Related Controls on Upward Hydrothermal Flow: An Integrated Geological Study of the Têt Fault System, Eastern Pyrénées (France), Geofluids, 2017, 1–19, https://doi.org/10.1155/2017/8190109, 2017.

Tesfaye, S., Rowan, M. G., Mueller, K., Trudgill, B. D., and Harding, D. J.: Relay and accommodation zones in the Dobe and Hanle grabens, central Afar, Ethiopia and Djibouti, JGS, 165, 535–547, https://doi.org/10.1144/0016-76492007-093, 2008.

Tong, H., Koyi, H., Huang, S., and Zhao, H.: The effect of multiple pre-existing weaknesses on formation and evolution of faults in extended sandbox models, Tectonophysics, 626, 197–212, https://doi.org/10.1016/j.tecto.2014.04.046, 2014.

Trudgill, B. and Cartwright, J.: Relay-ramp forms and normal-fault linkages, Canyonlands National Park, Utah, Geological Society of America Bulletin, 106, 1143–1157, https://doi.org/10.1130/0016-7606(1994)106<1143:RRFANF>2.3.CO;2, 1994.

Tveite, H.: The QGIS Line Direction Histogram Plugin, 2015.

Varet, J., Géraud, Y., Tarits, P., Sciullo, A., Contini, M., Nardini, I., Wheeler, W. H., Onyango, S., Rutagarama, U., Atnafu, B., Onjala, J., Moussa, K., Omenda, P., Gardo, I. A., and Change, Z.: The Geothermal Village Project (GV1) Supported by the LEAP-RE Research Programme Launched by the EU in Partnership with the AU, in: Proceedings of the 8th African Rift Geothermal Conference, Nairobi, Kenya, 11, 2020.

Walter, B., Géraud, Y., Hautevelle, Y., Diraison, M., and Raisson, F.: Fluid Circulations at Structural Intersections through the Toro-Bunyoro Fault System (Albertine Rift, Uganda): A Multidisciplinary Study of a Composite Hydrogeological System, Geofluids, 2019, 1–20, https://doi.org/10.1155/2019/8161469, 2019.

Whipp, P. S., Jackson, C. A.-L., Gawthorpe, R. L., Dreyer, T., and Quinn, D.: Normal fault array evolution above a reactivated rift fabric; a subsurface example from the northern Horda Platform, Norwegian North Sea, Basin Res, 26, 523–549, https://doi.org/10.1111/bre.12050, 2014.

World Bank: Rural population (% of total population) - Sub-Saharan Africa, The World Bank Group, accessed January 15, 2023a, https://data.worldbank.org/indicator/SP.RUR.TOTL.ZS?locations=ZG

World Bank: Access to electricity, rural (% of rural population) - Sub-Saharan Africa, The World Bank Group, accessed January 15, 2023b, https://data.worldbank.org/indicator/EG.ELC.ACCS.RU.ZS?locations=ZG&view=chart